Am J Physiol Lung Cell Mol Physiol 304: L489–L503, 2013.
First published January 25, 2013; doi:10.1152/ajplung.00181.2012.

Human bronchial epithelial cells exposed in vitro to cigarette smoke at the air-liquid interface resemble bronchial epithelium from human smokers

Carole Mathis,[1] Carine Poussin,[1] Dirk Weisensee,[2] Stephan Gebel,[2] Arnd Hengstermann,[2] Alain Sewer,[1] Vincenzo Belcastro,[1] Yang Xiang,[1] Sam Ansari,[1] Sandra Wagner,[1] Julia Hoeng,[1] and Manuel C. Peitsch[1]

[1]*Philip Morris International Research and Development, Philip Morris Product SA, Neuchâtel, Switzerland;* [2]*Philip Morris International Research and Development, Philip Morris Research Laboratories, Cologne, Germany*

Submitted 8 June 2012; accepted in final form 24 January 2013

Mathis C, Poussin C, Weisensee D, Gebel S, Hengstermann A, Sewer A, Belcastro V, Xiang Y, Ansari S, Wagner S, Hoeng J, Peitsch MC. Human bronchial epithelial cells exposed in vitro to cigarette smoke at the air-liquid interface resemble bronchial epithelium from human smokers. *Am J Physiol Lung Cell Mol Physiol* 304: L489–L503, 2013. First published January 25, 2013; doi:10.1152/ajplung.00181.2012.—Organotypic culture of human primary bronchial epithelial cells is a useful in vitro system to study normal biological processes and lung disease mechanisms, to develop new therapies, and to assess the biological perturbations induced by environmental pollutants. Herein, we investigate whether the perturbations induced by cigarette smoke (CS) and observed in the epithelium of smokers' airways are reproducible in this in vitro system (AIR-100 tissue), which has been shown to recapitulate most of the characteristics of the human bronchial epithelium. Human AIR-100 tissues were exposed to mainstream CS for 7, 14, 21, or 28 min at the air-liquid interface, and we investigated various biological endpoints [e.g., gene expression and microRNA profiles, matrix metalloproteinase 1 (MMP-1) release] at multiple postexposure time points (0.5, 2, 4, 24, 48 h). By performing a Gene Set Enrichment Analysis, we observed a significant enrichment of human smokers' bronchial epithelium gene signatures derived from different public transcriptomics datasets in CS-exposed AIR-100 tissue. Comparison of in vitro microRNA profiles with microRNA data from healthy smokers highlighted various highly translatable microRNAs associated with inflammation or with cell cycle processes that are known to be perturbed by CS in lung tissue. We also found a dose-dependent increase of MMP-1 release by AIR-100 tissue 48 h after CS exposure in agreement with the known effect of CS on this collagenase expression in smokers' tissues. In conclusion, a similar biological perturbation than the one observed in vivo in smokers' airway epithelium could be induced after a single CS exposure of a human organotypic bronchial epithelium-like tissue culture.

gene set enrichment analysis; organotypic culture; microRNA signature; smoking gene signature; translational systems toxicology

IN RECENT YEARS, A CLEAR SHIFT in the strategy of toxicological assessment of environmental agents has been started. In 2007, the U.S. National Research Council published a report developing a long range strategic plan to assess the potential toxic effect of environmental compounds (1). This new strategy responds in particular to the need of finding alternatives to animal testing (8). Facing the real difficulty to translate toxicological findings obtained in animal models to human context, scientists saw the urge of developing more reliable human in vitro systems.

Bronchial epithelial cells and epithelial lining fluid are the first line of defense to toxic gases and particles in the ambient air. Thus they are of particular interest to assess the biological impact of environmental air pollutants. Airway epithelial cells are also used in research to understand the biochemical and molecular mechanisms underlying some airway diseases such as asthma, cystic fibrosis (CF) and chronic obstructive pulmonary disease (COPD) (16). Human bronchial epithelial cells can be collected by brushing donor lungs during bronchoscopy procedure (70). They can then be cultured as a monolayer of undifferentiated bronchial epithelial cells or further developed into an organotypic pseudo-stratified bronchial epithelium-like tissue with an air-liquid interface (69, 70). Under the later condition, cells are differentiated and polarized. They develop tight junctions and show the typical characteristics of ciliated and nonciliated epithelial cells, goblet cells, and basal cells, which compose the lung bronchial epithelium in vivo (33). Those morphological properties already support the relevance of this cell culture model as a potential gold standard human airway assay. In addition, bronchial epithelial cells can be obtained from donors with different pathologies, and these air-liquid interface cultures are thus of special interest in the study of diseases mechanisms [e.g., asthma (18, 68, 73), COPD (55), CF (12, 50), and to develop and test new therapies (11, 21, 76)]. In addition to being such a valuable in vitro system for airway pathology investigation, it is also possible to study normal biological processes similar to those occurring in vivo in a healthy context. For instance, bronchial epithelial tissue-like cultures present the mucociliary morphology observed in human lung and so have been used to study the lineage, differentiation, and function of secretory cells to better understand the events leading to mucus hypersecretion (4, 52, 63). Others have taken advantage of this in vitro system to dissect molecular pathways activated in bronchial epithelial cells exposed to cytokines (5) or during inflammatory processes (24). Recently, Pezzulo et al. (46) compared the genome-wide expression profile of tracheal and bronchial human airway epithelia in vivo with the expression profile of primary human organotypic bronchial epithelium-like tissue culture. They demonstrated that, in addition to the morphological similarities previously reported, the transcriptional profile showed by this in vitro system specifically mimics that observed in healthy airway epithelial cells. This suggests that primary culture of differentiated normal human bronchial epithelial (NHBE) cells with an air-liquid interface can closely recapitulate the biology of human airway epithelium under normal conditions.

Another interesting feature of this airway culture system is the possibility to expose the cells directly to any gas, solid, and

Address for reprint requests and other correspondence: C. Mathis, PHILIP MORRIS International R&D, c/o Philip Morris Product SA, Quai Jeanrenaud 5, CH-2000 Neuchâtel, Switzerland (e-mail: Carole.Mathis@pmi.com).

  ISSN 1040-0605.

liquid substance suspended in the air. This is a clear advantage when investigating the impact of complex aerosol mixtures, such as cigarette smoke (CS). Indeed, the suitability of this 3D airway culture has been assessed for the screening of inhaled toxicants, including cadmium, nicotine, formaldehyde, and urethane (2). Other workers (35) have tested the gene expression changes after acute exposure to whole CS in this type of culture.

In the present study, we investigate the translatability of the CS-induced effect observed in cells directly exposed in vivo and in vitro. To this end, we used NHBE cells differentiated in an organotypic culture (AIR-100) and exposed them for various times at the air-liquid interface to either fresh air or mainstream CS in the Vitrocell system. We then combined microarray technologies (gene expression and miRNA) and a functional characterization to assess how well this in vitro system under CS exposure could imitate the biology of human smoker bronchial epithelium. Initially, five publicly available datasets were selected to derive three types of human bronchial epithelial cell gene signatures by using a supervised-machine learning approach. More precisely, four datasets were used to obtain a specific smoking gene signature (current smokers vs. nonsmokers) (3, 19, 56, 61); two datasets were used to obtain a smoking cessation gene signature (former smokers vs. current smokers) (3, 71); and one dataset was used for a low-CS-exposure gene signature (low CS exposure vs. nonsmokers) (61). To assess whether these three different types of in vivo gene signatures were enriched in the gene expression profile of CS-exposed AIR-100 culture, we performed a Gene Set Enrichment Analysis (GSEA) (62). We observed that even a single exposure of whole CS could induce in AIR-100 culture a similar system response profile to the one observed in vivo in human lungs inhaling CS. We then investigated whether other biological processes known to be affected by CS in the human bronchial epithelium were also perturbed within the in vitro system we used.

miRNAs are a major class of small noncoding RNAs. They posttranscriptionally act as negative regulators of their target genes, which are expected to cover as much as one-third of the human transcriptome (28). In lungs, miRNAs have been shown to be differentially regulated in response to a wide variety of physiological and environmental stimuli and to be disturbed in many disease states, giving rise to characteristic expression profiles (65). Even if the availability of miRNA data from bronchial epithelial cells obtained by brushing is limited (only one published in vivo dataset from smokers and nonsmokers published; Ref. 54), we analyzed miRNA expression changes induced by CS exposure in the 3D airway tissue culture system and compared it with the in vivo miRNA signature obtained from Schembri et al. (54).

Finally, we also measured the release of MMP-1, the expression of which has been shown to be upregulated by CS both in vivo and in vitro (10, 36, 38). We observed a clear CS dose-dependent increase of the release of pro-MMP-1 protein by exposed AIR-100 culture.

Altogether, our results suggest that differentiated NHBE cells cultured at the air-liquid interface and exposed to a single exposure of CS recapitulate many of the biological perturbations observed in the airway epithelium of smokers.

MATERIALS AND METHODS

Primary Organotypic Culture of Human Bronchial Epithelial Cells

EpiAirway tissues (AIR-100) were obtained from MatTek (Ashland, MA). The donor of the primary bronchial epithelial cells was a 23-yr-old male with no smoking history. In a cell culture insert, NHBE cells are grown and differentiated on a porous membrane support, allowing an air-liquid interface with warmed culture medium below the cells and a gaseous test atmosphere above them (see Fig. 1). Tissue insert integrity was controlled by *1*) the absence of medium leakage and *2*) by transepithelial electrical resistance (TEER). Measurement of TEER provides an indirect measure of tight junction formation and is often used as a marker of epithelial layer disruption (43). Cell viability was assessed 24 h after exposure using the soluble tetrazolium salt resazurin (Sigma, Taufkirchen, Germany) (40, 48).

CS Preparation and Vitrocell Exposure

Tissues were exposed for 7, 14, 21, and 28 min at the air-liquid interface to either synthetic air (85% nitrogen and 15% oxygen; Praxair, Düsseldorf, Germany) or to 15% (vol/vol) mainstream CS in the Vitrocell system (Fig. 1) (S Weber, M Hebestreit, unpublished observations). Seven puffs per cigarette and one puff per minute of exposure were used for all conditions, and the number of cigarettes varied to adjust to the exposure times. The Total Particulate Matter and CO dose inside the exposure chamber have been estimated to 7.74 μg and 8.3 μg per well per minute of exposure, respectively. The reference cigarette 3R4F was obtained from the University of Kentucky (www.ca.uky.edu/refcig) and was smoked on the VC 10 smoking robot (Vitrocell, Fig. 1*A*) in basic conformity with the International Organization for Standardization smoking regimen (ISO 2000). After exposure, the tissues were incubated with fresh culture medium for 0.5, 2, 4, 24, and 48 h before further analysis.

Pro-MMP-1 Quantification

The quantikine human pro-MMP-1 immunoassay (R&D Systems, Minneapolis, MN) was used for the quantitative determination of pro-MMP-1 concentrations in cell culture medium harvested 48 h after exposure. Absorbance was measured at 450-nm wavelength using a Fluostar Optima plate reader (BMG Labtech, Durham, NC).

RNA and Microarray Hybridization

Exposed tissues were lysed at the different postexposure time points using Qiazol lysis reagent (Qiagen, Valencia, CA). miRNeasy Mini Kit (Qiagen) was used to extract and purify both mRNAs and miRNAs. The quality of the total RNAs was verified by an Agilent 2100 Bioanalyzer profile. A RIN number greater than 8 was required. For mRNA analysis, 100 ng of total RNA were processed as described in the GeneChip HT 3′ IVT Express User Manual (Affymetrix), and Genechip high-throughput Human Genome U133 Array Plates were used for hybridization. For miRNA analysis, the following reference sample was used: FirstChoice Human Total RNA Survey Panel, made of RNAs from different tissues of multiple individuals (catalog no. AM6000; Ambion, Austin, TX). 500 ng of total RNA from sample and reference were labeled using miRCURY LNA Array power labeling kit (Exiqon, Vedbaek, Denmark). The Hy3-labeled samples and a Hy5-labeled reference RNA sample were mixed pairwise and hybridized in randomized order to the miRCURY LNA Array version 5th Generation (Exiqon), which contains capture probes targeting all miRNAs for human, mouse, or rat registered in the miRBASE version 15.0 at the Sanger Institute. The hybridization was performed using a Tecan HS4800 hybridization station (Tecan, Vienna, Austria). The miRCURY LNA array microarray slides were scanned using the Agilent G2565BA Microarray Scanner System (Agilent Technologies, Santa Clara, CA), and the image analysis was carried out using the ImaGene 9.0 software (BioDiscovery, Hawthorne, CA).

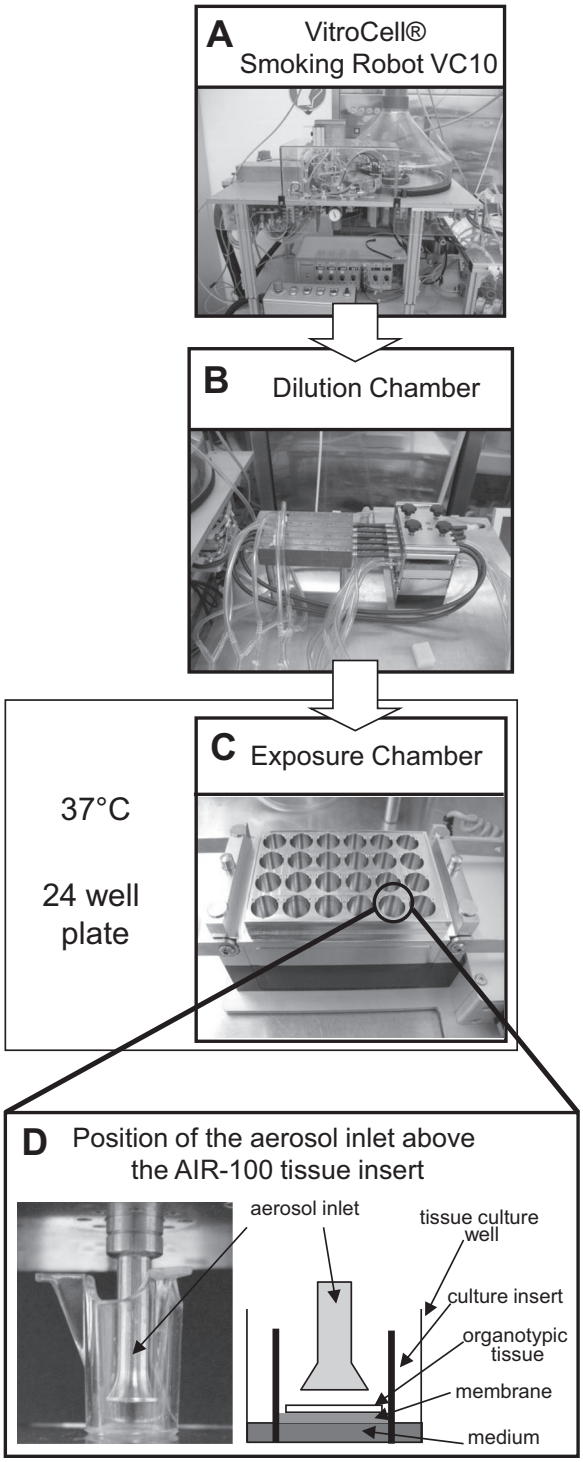

Fig. 1. Schematic representation of the whole cigarette smoke (CS) exposure system and the exposure chamber. In the Vitrocell VC10 smoking robot (*A*), 3R4F cigarettes produce discontinuously whole CS (15% CS vol/vol with synthetic air) at the rate of 1 puff/min per cigarette. CS then enters the dilution chamber (*B*) (35 ml/8 s), where it is mixed continuously with synthetic air (0.2 to 0.5 l/min). The flow of diluted CS passes then in the exposure chamber (*C*), where the cell culture inserts are placed just underneath the aerosol inlet (*D*) during the defined length of exposure. In a cell culture insert, normal human bronchial epithelial (NHBE) cells are grown and differentiated on a porous membrane support, allowing an air-liquid interface with warmed culture medium below the cells and a gaseous test atmosphere above them.

Gene Expression Microarray Data Processing and Analysis

Raw data were background corrected, normalized, and summarized using the GCRMA algorithm (74). Quality control check of all chips was done with different R packages from the Bioconductor (affy, affyPLM) (58). One chip (sham/14-min exposure/48-h postexposure) was excluded from further analysis due to its higher intensity signal variability reflected by much higher NUSE median and interquartile range compared with other chips and a lower correlation coefficient. Probe sets with low signal across all conditions (95th percentile of $\log_2$ expression distribution below 7) were filtered out. Gene expression data obtained from CS-exposed AIR-100 experiments were submitted to ArrayExpress with the following accession numbers: *1*) E-MTAB-874 for the mRNA dataset and *2*) E-MTAB-877 for the miRNA dataset. To identify probe sets with a modulated expression on CS treatment dependently or independently of exposure time (considered as a dose variable) and/or postexposure time, a linear model was defined as described below (*Eq. 1*) and computed for each postexposure time. This model included the treatment variable (2 levels: sham and smoke), the dose variable (4 levels: 7, 14, 21, 28 min), and the interaction of both variables. ϵ corresponded in the formula to normally distributed random noise. *Equation 1* is as follows: Expression $\sim \beta_0 + \beta_t \cdot$Treatment + $\beta_d \cdot$Dose + $\beta_i \cdot$Treatment * Dose + ε. All β coefficients that represent the effects of interest described above were estimated using the limma R package (58, 59).

MicroRNA Microarray Data Processing and Analysis

Raw data were normalized following Exiqon Hy3 single color pipeline consisting of a local background subtraction (normexp with offset value 10) (51), standard quantile normalization, and median summarization. Quality control check of all chips was performed based on the variability of the available control probes and on the between-array correlations of the miRNA probe sets. Four chips needed to be excluded from further analysis: one due to low RNA quality (sham/21-min exposure/48-h postexposure) and three (1: CS/7-min exposure/24-h postexposure; 2: CS/14-min exposure/4-h postexposure; 3: sham/14-min exposure/48-h postexposure) because they were outliers (because their hybridization signals displayed an abnormally high variability compared with the other arrays). miRNA probe sets that were not detected in at least one chip were excluded, the detection threshold being fixed by Exiqon as the 5% percentile of all probe signals measured on a given array. As a result, 229 miRNA probe sets were considered for further analysis. Additionally, a correction of the normalized expression values for possible batch effects resulting from the hybridization factors was performed using the ComBat package (6). For the identification of differentially expressed miRNAs on CS treatment, the same linear model was considered as for mRNA (*Eq. 1*) in the previous paragraph. Using additionally centered values for the treatment ($-1/2$ and $1/2$, for sham and smoke, respectively) and the dose variables (-10.5, -3.5, 3.5, 10.5) gives the following expression for the CS-induced differential expression (*Equation 2*): Differential Expression = Expression(smoke) − Expression(sham) $\sim \beta_t + \beta_i \cdot$* Dose + ε. The above choice of modified values for the treatment and dose variables enables interpreting β_t as the dose-independent part of the CS-induced differential expression. Similar to mRNA analysis, the linear model coefficients β_t and β_i and the corresponding *P* values were computed using the limma R package (58, 59).

Computational In Vivo/In Vitro Translational Analysis

Generation of the in vivo smoking and smoking cessation gene signatures. Four relevant human gene expression datasets [GSE4498: Harvey et al. (19); GSE20257: Shaykhiev et al. (56); GSE7895: Beane et al. (3); and GSE19667: Strulovici-Barel et al. (61)] were identified in the Gene Expression Omnibus (GEO) database. We also selected the dataset published by Zhang et al. (71), which was kindly shared by

the authors upon our request. Briefly, these datasets included gene expression profiles from bronchial epithelial cells obtained from nonsmokers, current smokers, and former smokers (3, 71), all healthy. A supervised-machine-learning approach including SAM (66) and a support vector machine (9) was applied in a 10-fold cross-validation procedure to extract a specific and robust human smoking (current smokers vs. nonsmokers; GSE4498; GSE20257, GSE7895) and smoking cessation (former smokers vs. current smokers; GSE7895 & Zhang's dataset) gene signature. Both smoking and low exposure to CS gene signatures were directly extracted from Strulovici-Barel et al. (61) because complete raw data were not available.

Generation of the in vivo smoking miRNA signature. The relevant dataset is available in the GEO database [GSE14634: Schembri et al. (54)]. It contains the miRNA profiles of human bronchial epithelial cells obtained by bronchoscopy from never and current smokers, all healthy at the time of sampling. Hybridization of the isolated small RNAs was performed on the Invitrogen NCode microarray. The corresponding normalized expression matrix (series matrix) was directly downloaded from GEO. After quality control, 3 outlying arrays were excluded, leaving 19 samples corresponding to 9 current and 10 never smokers. A filter was also applied on the miRNA probe sets, based on an array-specific detection threshold given by the 99th quantile of the intensity values measured on the blank probe sets. Taking only the miRNAs that are detected in at least half of the samples of one group left exactly 232 probe sets, similarly to the original work by Schembri et al. (54). The in vivo smoking miRNA signature was then calculated based on a pairwise comparison between the two groups using the Welsh's *t*-test implemented in the function Mattest from the MATLAB Bioinformatics toolbox. Applying a *P* value threshold of 0.05 yielded a strongly asymmetric signature constituted of 2 upregulated and 35 downregulated miRNAs.

Gene set enrichment analysis. To compare the in vivo smoking and smoking cessation gene signatures with the in vitro AIR-100 expression profiles over postexposure time points, GSEA was done with full contrasts computed for the treatment effect independently of the dose (62). For each postexposure time, the list of genes was decreasingly sorted by the *t*-values associated to the β_t coefficient. Normalized enrichment scores with an associated false discovery rate (FDR) ≤ 0.05 were considered to be statistically significant. The functional analysis has been performed using the GSEA website from the broad institute of MIT and Harvard: http://www.broadinstitute.org/gsea/index.jsp. To investigate the biological functions associated with our list of genes of interest, we computed their overlap with known gene sets like KEGG, BIOCARTA, and REACTOME. We also identified the target genes regulated by the transcription factor Nrf2 using Ingenuity.

Statistics

The degree of agreement between smoking or smoking cessation gene signatures was measured with the Fleiss κ statistic. The measure calculates the degree of agreement in classification over that which would be expected by chance and is scored as a number between 0 and 1 (14).

RESULTS

To assess how closely an in vitro assay can mimic the biological effect of CS observed in lung epithelium of smokers, we used the following experimental system: NHBE cells were obtained from a healthy adult nonsmoking donor. Cells were differentiated into an organotypic airway epithelium (named by the supplier: AIR-100) with an air-liquid interface (Fig. 1). NHBE cells cultured in this condition develop many of the typical characteristics observed in human lung bronchial epithelium (33, 69, 70). They formed a pseudo-stratified bronchial epithelium-like tissue and displayed the morphological characteristics of the four main cell types that constitute human lung epithelium: ciliated (Fig. 2*A*) and nonciliated cells (Fig. 2*C*), goblet cells (Fig. 2*B*) located at the apical side, and p63-positive basal cells (Fig. 2*C*). In addition, the presence of an air-liquid interface allows a direct exposure of the organotypic tissue with fresh mainstream whole CS. By using the Vitrocell exposure system, the airway culture is maintained in an appropriate humidified and temperature controlled atmosphere and is exposed directly at the apical surface with the test aerosols. This setup offers the advantage of avoiding solution or aerosol losses or dissolution and excludes reactions of constituents with the medium (Fig. 1*D*).

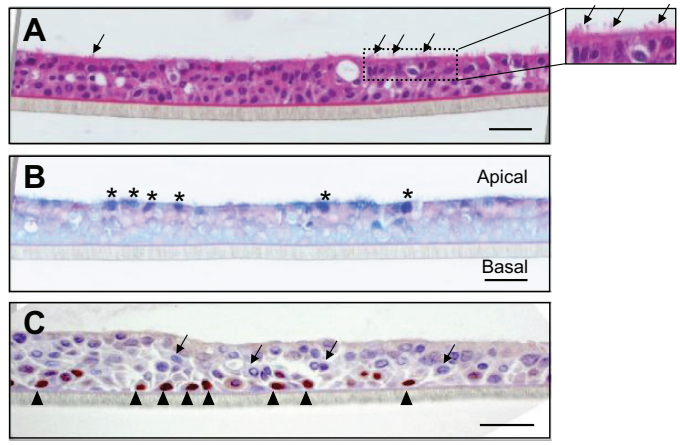

Fig. 2. Morphology of primary organotypic culture of human bronchial epithelial cells showed after Hematoxylin/Eosin staining (*A*), Alcian Blue-Periodic Acid Schiff staining (*B*), and p63 immunostaining (*C*). As observed in vivo, this in vitro culture model forms a multilayered pseudo-stratified epithelium composed of ciliated cells (*A*, arrows indicating cilia), nonciliated cells (*C*, arrows indicating p63-negative nonciliated epithelial cells), goblet cells located on the apical side (*B*, asterisks), and basal cells (*C*, arrow heads indicating p63-positive basal cells). Scale bar equals 30 μm.

AIR-100 tissue cultures were exposed once to CS over different times (7, 14, 21, 28 min) and per exposure time; four postexposure times (0.5, 2, 4, 24, 48 h) were investigated (Table 1). To perform a thorough comparison with the in vivo situation, multiple endpoints (gene expression and miRNA profiles, MMP-1 release, immunostaining, and histology) have been captured at the different postexposure time points (Table 1).

Enrichment of Human Smoking Gene Signatures in CS-Exposed AIR-100 Tissue Culture

The focus of our study was to determine whether the perturbation induced by CS observed in the epithelium of smokers' airways is reproducible in an in vitro system (the AIR-100 tissue culture) recapitulating most of the characteristics of this lung epithelium. To test this hypothesis, we used GSEA (62) as a well-established method to quantify biological similarities between experiments (29). We thus assessed the enrichment of human smoking gene signatures derived from four transcriptomic studies (3, 19, 56, 61) in the gene expression profiles of AIR-100 exposed to whole CS compared with sham (details in MATERIALS AND METHODS). Even though the origin of the bronchial epithelial cells analyzed in these four studies was different [large airway (3); small airway (19, 56, 61)], the response to CS has been demonstrated to be homogeneous throughout the bronchial epithelium (15, 19). It is noteworthy that samples from the three studies using cells derived from the small airway are overlapping to some extent

Table 1. *Study design and summary of all biological measurements performed along the experiment*

Test Substance	SHAM				Cigarette Smoke			
Exposure time, min	7	14	21	28	7	14	21	28
PE Time, h	0.5	0.5	0.5	0.5	0.5	0.5	0.5	0.5
	2	2	2	2	2	2	2	2
	4	4	4	4	4	4	4	4
	24	24	24	24	24	24	24	24
	48	48	48	48	48	48	48	48
Viability, test at PE time	4	4	4	4	4	4	4	4
	24	24	24	24	24	24	24	24
		48		48		48		48
Gene Expression, all PE time	√	√	√	√	√	√	√	√
miRNAs, all PE time	√	√	√	√	√	√	√	√
Pro-MMP-1 Release	48	48	48	48	48	48	48	48
Immunostaining/Histology	24	24	24	24	24	24	24	24
		48		48		48		48

PE, postexposure; MMP, matrix metalloproteinase.

(see Fig. 3*C*) and may therefore contribute to the low difference observed between the various comparison performed between each of these in vivo datasets and our in vitro dataset. In fact, the comparison of these four smoking gene signatures revealed a fair gene overlap as defined by the calculated Fleiss κ statistic of 0.38 and 0.27, respectively: 37 genes upregulated and 10 genes downregulated in common (Fig. 3 and Supplemental Table S1 for details; supplemental material for this article is available online at the *American Journal of Physiology Lung Cellular and Molecular Physiology* website). A heatmap of the expression level of the leading-edge genes belonging to the in vitro dataset and present in the smoking gene signatures obtained from the different in vivo datasets is available in Fig. 4.

CS-exposed AIR-100 gene expression profiles obtained for each postexposure time were sorted by the moderated *t* values associated to the β_t coefficient present in the linear model (see *Eq. 1*) and computed for each gene. This β_t coefficient estimated the effect of CS exposure independent of the dose (or the exposure time) and better mimics the heterogeneity observed in a group of active smokers having variable cigarette consumption.

GSEA results for each smoking gene signature tested are represented in Fig. 5. The directionality of the differentially regulated genes of the CS-exposed AIR-100 tissue always matches the directionality of the human smoking gene signatures where a significant normalized enrichment score was observed. For all four signatures, we found a similar pattern of enrichment score in the CS-exposed AIR-100 upregulated genes set with the highest score at 4-h postexposure time and a lower score after 24-h postexposure time (Fig. 5, *A*, *C*, *E*, and *G*). Moreover, this enrichment was still significant (at least FDR ≤ 0.05) at the 48-h postexposure time point. On the other hand, no significant enrichment score was observed after 30-min postexposure (for either up- or downregulated gene sets), suggesting that an enrichment of the human smoking gene signatures start to appear significant only 2 h after CS exposure in the AIR-100 in vitro system. We also noticed that, in the downregulated gene set of CS-exposed AIR-100, the four smoking gene signatures were significantly enriched mainly at 2- and 4-h postexposure time (Fig. 5, *B*, *D*, *F*, and *H*). Interestingly, for the smoking gene signatures derived from Shaykhiev et al. (56) and from Strulovici-Barel et al. (61), we also observed a sustained enrichment in the AIR-100 downregulated genes set 24 h and 48 h after CS exposure, respectively.

Recently, the whole genome transcriptome of small airway epithelium samples obtained from individuals with low CS exposure was assessed to identify those genes that were most sensitive to tobacco smoke (61). Figure 5, *I-J*, represents the GSEA results of this low CS exposure gene signature in the CS-exposed AIR-100 gene sets. An enrichment score similar to the one obtained for the previous smoking upregulated gene signature was observed for each postexposure time analyzed. On the contrary, the low CS exposure downregulated gene signature was not significantly enriched in the downregulated genes of the AIR-100 tissue expression profile at any postexposure time point. Thus CS exposure induces a comparable pattern of upregulated genes in both in vitro and human airway epithelium even if the exposure level is high (current smokers) or low (low CS exposure and in vitro single exposure).

Negative Correlation of Smoking Cessation Gene Signatures in CS-Exposed AIR-100 Tissue Culture

Various studies have shown that most of the genes that are upregulated in a smoker's airway epithelium (compared to nonsmokers) revert after a smoking cessation period of few months to a level similar to that observed in nonsmokers (3, 15, 60). Our results strongly suggest that one single CS exposure triggers in AIR-100 tissue a response similar to the one observed in vivo in the lung of smokers, at least at the RNA level. Based on this observation, we decided to investigate whether an in vivo smoking cessation gene signature could be enriched in the gene expression profile of our in vitro system after CS exposure. Two datasets of human bronchial epithelial cells obtained from former smokers vs. current smokers and published by Zhang et al. (71) and Beane et al. (3) were used to derive a gene signature with the same approach described previously for the smoking gene signature generation (see MATERIALS AND METHODS). These two in vivo gene signatures represent the genes whose expression is reversed following smoking cessation compared with smoking status. The overlap found between the two smoking cessation gene signatures corresponded to a light agreement (Fleiss κ statistic of 0.02 and 0.06 for up- and downregulated genes, respectively) for the downregulated genes, where 19 were common between the two

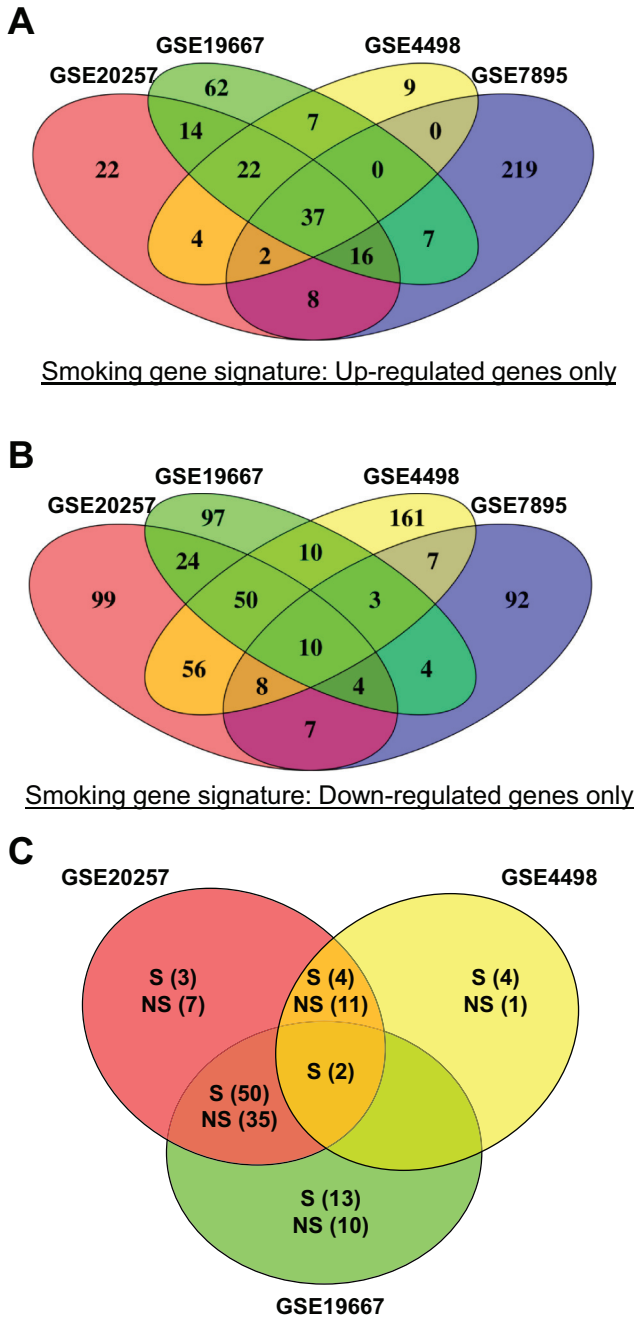

Fig. 3. Venn diagrams representing the overlapping upregulated (*A*) and downregulated (*B*) genes present in the 4 in vivo smoking gene signatures used in the Gene Set Enrichment Analysis (GSEA). *C*: Venn diagram representing the overlapping samples (S, smokers; NS, nonsmokers) from 3 of the 4 in vivo datasets used in this study. No overlapping samples were found between the dataset GSE7895 and the other in vivo datasets. The following authors used the following genes: Shaykhiev et al. (56), GSE20257; Harvey et al. (19), GSE4498; Beane et al. (3), GSE7895; and Strulovici-Barel et al. (61), GSE19667.

datasets against only 3 for the upregulated ones (see Supplemental Table S1 for more details).

With the exception of 0.5-h postexposure time point, we observed a significant enrichment of the genes that were downregulated (GS DN; Fig. 6, *A* and *C*) following a smoking cessation period in the most upregulated genes in CS-exposed AIR-100 tissue. Enrichment of cessation-induced upregulated genes (GS UP; Fig. 6, *B* and *D*) was only observed in the most downregulated genes in AIR-100 (AIR-100 DN) at 0.5-h and 2-h postexposure time and only for Beane's smoking cessation gene signature (Fig. 6*B*). Overall, the enrichment significance levels obtained for these smoking cessation gene signatures across the different postexposure time were much lower than the ones observed for smoking signatures. However, these results showed that some genes induced by CS in AIR-100 have a reversed expression profile following smoking cessation as observed in vivo in human bronchial epithelium studies (see Supplemental Table S2).

Functional Analysis

Because the highest enrichment scores were mostly found in the AIR-100 tissue culture at the 4-h postexposure time point (Figs. 5 and 6), the genes that contributed to these enrichment scores (leading edge genes) were extracted from GSEA results to investigate associated biological functions. Supplemental Table S2 contains three lists of leading edge genes that correspond to *1*) the upregulated genes in AIR-100 tissue expression profiles matching the in vivo smoking upregulated gene signatures, *2*) the upregulated genes in AIR-100 tissue expression profiles matching the in vivo smoking cessation downregulated gene signatures, and *3*) the downregulated genes in AIR-100 tissue expression profiles matching the in vivo smoking downregulated gene signatures. Using different biological sources of information (KEGG, Biocarta, and Reactome), an over-representation analysis of these three lists of genes highlighted various biological processes affected by CS exposure.

First, upregulated AIR-100 leading edge genes from in vivo smoking upregulated gene signatures contain genes coding for proteins involved in: *1*) the metabolism of xenobiotics by cytochrome P450 (e.g., CYP1A1, CYP1B1, CYP4F3, UGT1A10, ALDH3A1, and ALDH1A3), *2*) the redox balance (e.g., AKR1B10, AKR1C1, AKR1C2, AKR1C3, TXNRD1, TXN, and CBR3), *3*) the glutathione metabolism (e.g., GCLC, GCLM, and SLC7A11), and *4*) the pentose phosphate pathway (e.g., PGD, TALDO1, TKT, and G6PD) and solute transport activity (SLC7A11, SLC2A1, SLC6A6, SLC31A1, and SLC3A2). Many of those genes are also known to be direct targets of Nrf2 transcription factor (e.g., NQO1, TXNRD1, GCLM, ME1, TXN, GCLC, ABCC1, AKR1C1, FTH1, FTL, and SLC7A11) (information retrieved from Ingenuity).

Second, we found similar genes and consequently same biological functions associated to the upregulated leading edge genes of AIR-100 tissue from both in vivo smoking cessation downregulated gene signatures (Supplemental Table S2) and the upregulated in vivo smoking gene signatures (Supplemental Table S2). In particular, genes associated to the metabolism of xenobiotics by cytochrome P450 to the redox balance or to the pentose phosphate pathway are upregulated after CS exposure both in vivo and in vitro but are also seen downregulated in the lung of former smokers, suggesting their reversibility after smoking cessation. The upregulation of some of these genes (e.g., ALDH3A1, CYP1A1, CYP1B1, GCLC, and NQO1) was confirmed by RT-qPCR in AIR-100 tissue exposed for 28 min to CS and after 4 h of postexposure time (Table 2).

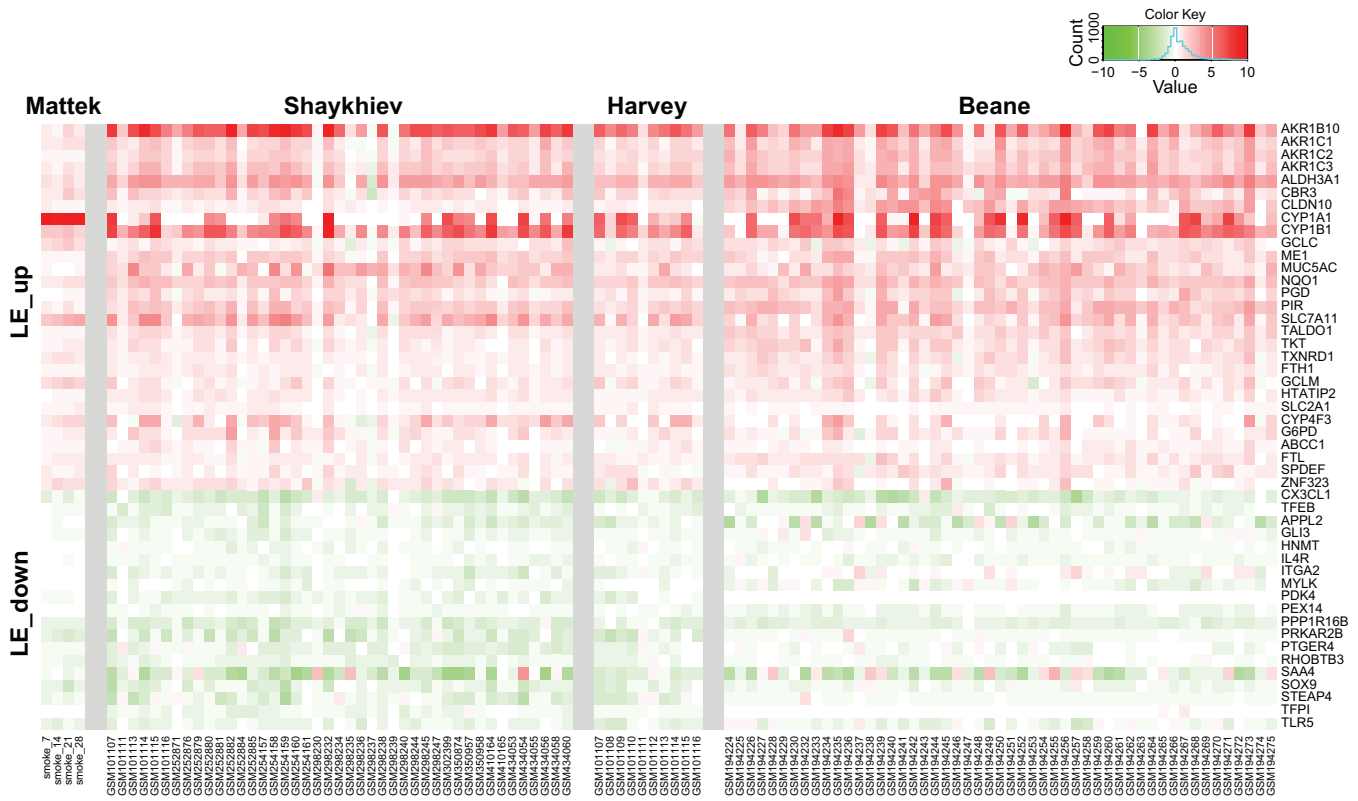

Fig. 4. In vitro/in vivo side-by-side heatmap for the leading edge (LE) genes. Heatmap of the fold changes for in vitro up- and downregulated LE genes are plotted side by side with extracted fold changes from in vivo studies [Shaykhiev et al. (56), Harvey et al. (19), Beane et al. (3)]. Fold changes from in vivo studies are obtained by taking the log2 of the gene expression ratio between smokers' samples (column of the matrix) against the average expression level from nonsmokers within the same study. AIR-100 (MatTek) fold changes are obtained similarly for each exposure time.

Finally, we found in both in vivo and in vitro context a downregulation of genes involved in the Notch pathway (DLL1, JAG2, MAML3, and HEY1), in the Shh pathway (GLI3 and PRKAR2B), in the family of apical junction complex molecules (CLDN8, CGN, OCLN, and PVRL3), and in the WNT/β-catenin pathway (SOX9, RHOU, and RUNX2).

CS Exposure Affects the Expression Profiles of miRNAs in Bronchial Epithelial Cells Both in Humans and In Vitro in a Similar Way

miRNAs are small noncoding RNAs known to play an important role in the regulation of gene expression. Recently, the impact of environmental chemicals on miRNA regulation of gene expression has been investigated (25). Although so far only one study (54) has reported the measurement of miRNA expression in bronchial epithelial cells from healthy smokers and nonsmokers, we analyzed miRNA CS-induced differential expressions in AIR-100 culture and performed an in vivo/in vitro comparison as follows: the Schembri et al. dataset (54) was used to construct an in vivo smoking miRNA signature constituted of 35 miRNAs (out of 232 detected probe sets) (see MATERIALS AND METHODS). In the present in vitro study, the differential expression of CS-induced miRNAs is most adequately determined using linear models following the multifactorial experimental design (see Table 1). Collecting all probe sets for which either β_t or β_i are statistically significant (corresponding P value < 0.05) yields a set of 118 miRNAs (out of 229 detected probe sets). Taken out of 232 and 229 detected probe sets, 110 human miRNA probe sets are detected in both cases, among which 14 miRNAs belong to the in vivo smoking miRNA signature.

Figure 7 shows how these 14 miRNAs behave in the in vitro conditions, revealing a global downregulation common to both in vitro and in vivo cases, as well as a subset of highly translatable miRNAs such as hsa-miR-106b/125b/146a/146b/148. Figure 7*A* displays the strongest moderated t statistic of each of the 110 commonly detected miRNAs, i.e., the moderated t statistics associated to the β_t or β_i coefficients of the linear models computed for the five postexposure time points that has the largest absolute value. In agreement with the in vivo results of Schembri et al. (54), the effect of smoke on miRNA expression consists in a strong downregulation for a large majority of the cases (91 out of 110). This is in particular the case for all 14 elements of the in vivo smoking miRNA signature, with five of them mentioned above appearing in the 20 highest ranked, leading to a good enrichment statistic (hypergeometric P value $= 0.08$). Beside confirming the in vitro/in vivo translatability, the results obtained here also provide stratification of the miRNA response based on its kinetics. As shown in Fig. 7*B*, not all miRNAs from the in vivo smoking signature react in the same way over postexposure time. Some are early responders (hsa-miR-24/106a/130a), some respond after 24 h only (hsa-miR-125b/148b), and some display a delayed but sustained response (hsa-miR-146a/b). These responses are sometimes further modulated by the exposure time captured by the β_i coefficients of the linear

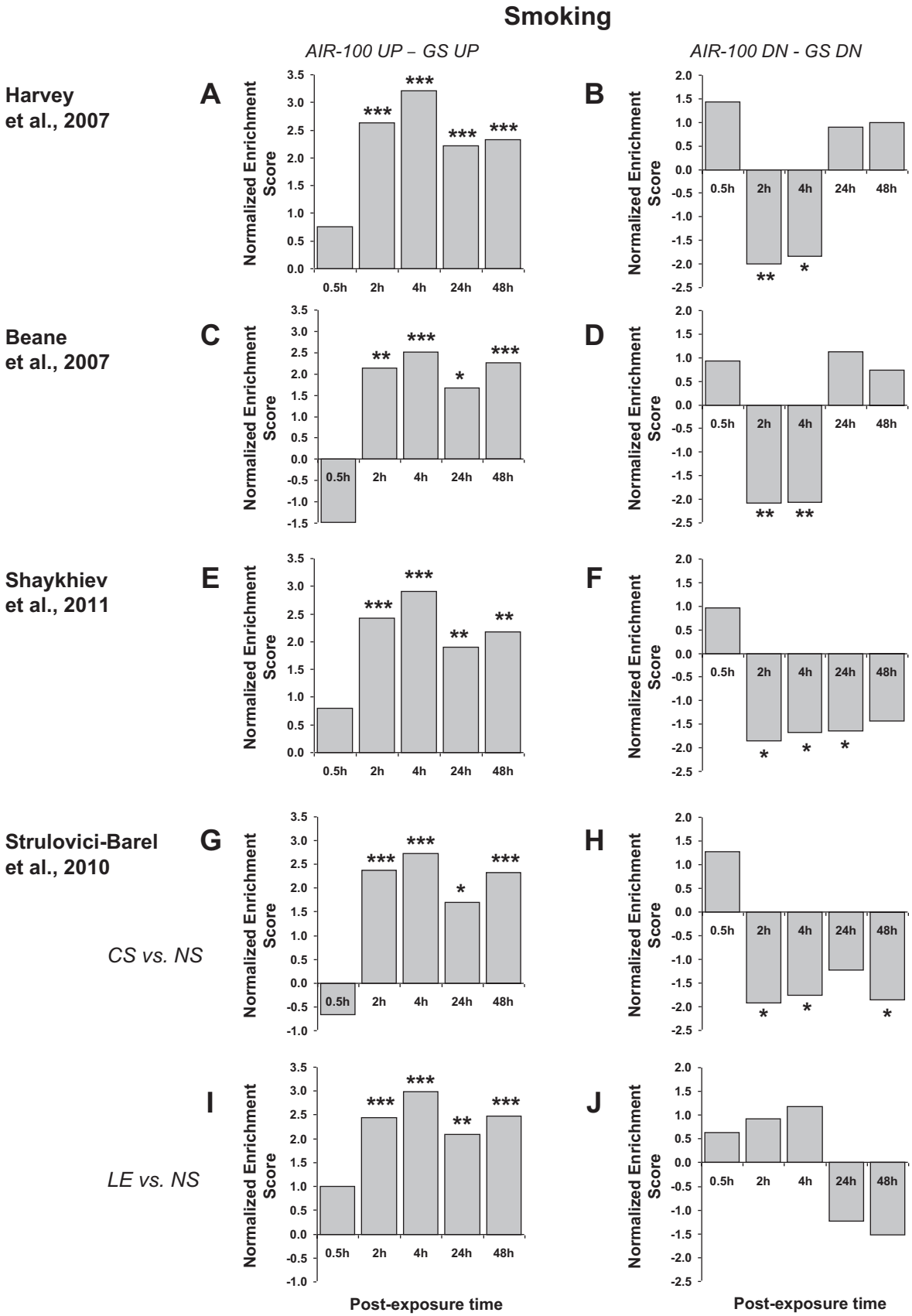

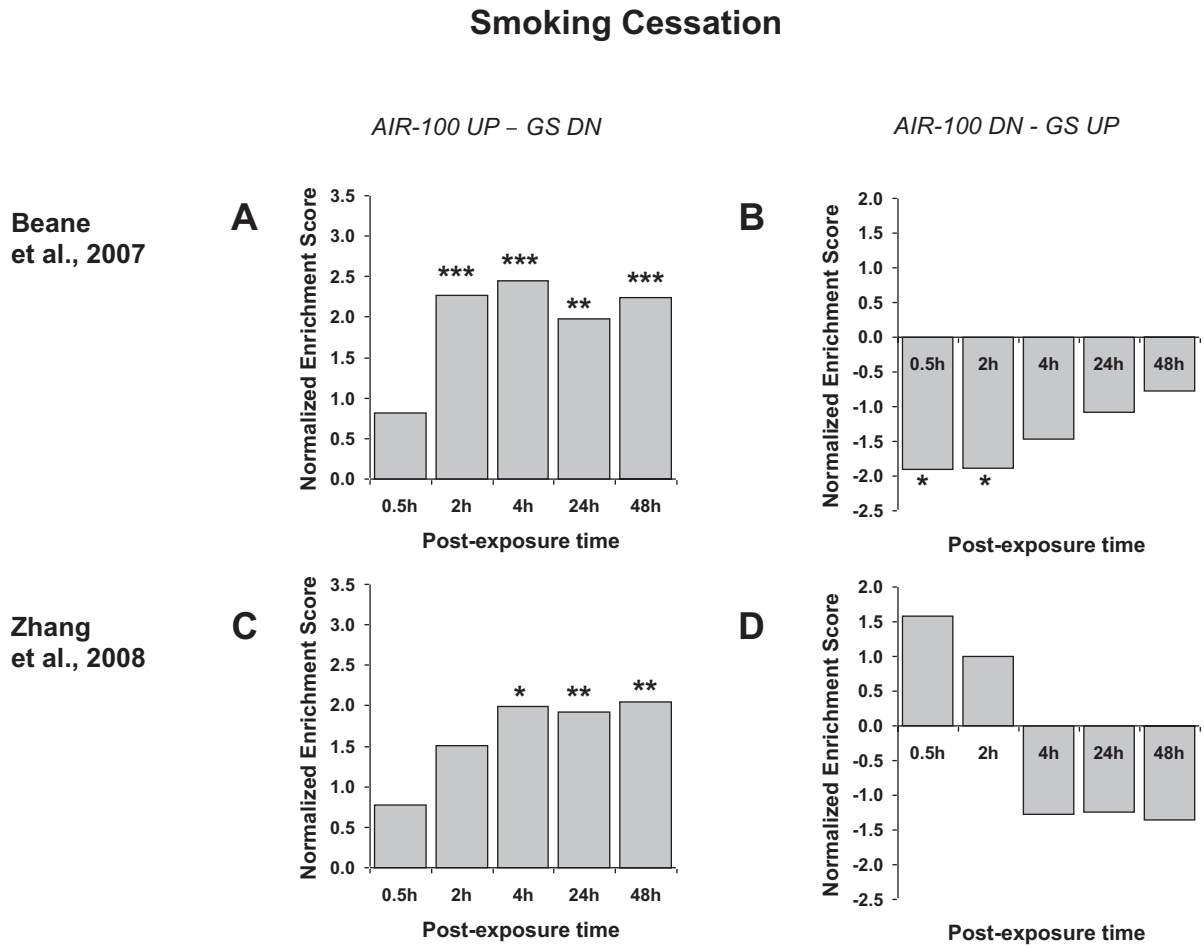

Fig. 6. In vivo smoking cessation downregulated gene signature is found significantly enriched in the upregulated leading edge of CS-exposed AIR-100 tissue. The GSEA approach was again used to assess the enrichment of genes derived from in vivo smoking cessation gene signatures (former smokers vs. current smokers) in the transcriptomic profiles of CS-exposed AIR-100 tissue after different postexposure time. Two in vivo smoking cessation gene signatures [Beane et al. (3) (*A*, *B*) and Zhang et al. (71) (*C*, *D*)] were tested for enrichment independently against ranked gene expression profiles from AIR-100. Normalized enrichment score computed for each postexposure time points are represented in *A–D* bar plots. Both gene signatures were split into upregulated and downregulated GS (GS UP and GS DN). ***FDR ≤ 0.0002; **FDR ≤ 0.01; *FDR ≤ 0.05.

models. An example is hsa-miR-148b that decreases after 24 h only at longer exposure times.

Smoking Induces MMP-1 Expression Both In Vivo and In Vitro in CS-Exposed-AIR-100 Tissue Culture

As a control for the responsiveness of our organotypic airway culture to CS exposure, we chose to measure in the culture medium the MMP-1, an interstitial collagenase known to be secreted by bronchial epithelial cells. This protein plays a role in tissue remodeling and repair during development and inflammation. Various studies have demonstrated the influence of CS on MMP-1 mRNA and protein expression (34, 36, 47). In addition, Mercer et al. (38) also identified a cigarette smoke-responsive region in the distal human MMP-1 promoter. A dose-dependent increase of pro-MMP-1 secretion (up to 14-fold) was observed 48 h after 14, 21, and 28 min of CS exposure (Fig. 8). This result demonstrates a similar capability of human bronchial epithelial cells cultured at the air-liquid interface to respond to CS exposure by releasing MMP-1 to what has been described previously in the tissue of human smokers.

DISCUSSION

Dissecting the biological perturbation induced by a complex hazardous aerosol mixture such as CS and trying to understand

Fig. 5. In vivo smoking gene signatures derived from airway epithelium transcriptomes are significantly enriched in CS-exposed AIR-100 tissue. The GSEA approach was used to assess the enrichment of genes derived from in vivo smoking gene signatures in the transcriptomic profiles of CS-exposed AIR-100 tissue after different postexposure time. Bar plots in *A–J* exhibit the normalized enrichment score computed for each postexposure time point. The gene set (GS) used to perform GSEA included smoking gene signatures from Harvey et al. (19) (*A*, *B*), Beane et al. (3) (*C*, *D*), Shaykhiev et al. (56) (*E*, *F*), and Strulovici-Barel et al. (61) (*G*, *H*). *I* and *J* correspond to GSEA performed with the low-CS-exposure signature. Low exposure (LE) vs. nonsmoker (NS). Each signature was split into upregulated (GS UP) and downregulated GS (GS DN). They were tested for enrichment independently against ranked gene expression profiles of CS-exposed AIR-100 tissue. Enrichments observed among the most significantly up- or downregulated genes in AIR-100 tissue were indicated by "AIR100 UP" and "AIR100 DN". ***False discovery rate (FDR) ≤ 0.0002; **FDR ≤ 0.01; *FDR ≤ 0.05.

Table 2. *Validation by RT-qPCR of the expression level of selected genes found upregulated after CS exposure in AIR-100 tissue culture and also identified in in vivo smoking gene signatures*

Gene Name	Assay ID Applied Biosystems	Exposure Time, min	PE, h	Fold Change	*P* Value
ALDH3A1	Hs00964880_m1	28	4	1.57	0.04959
CYP1A1	Hs00153120_m1	28	4	1068.69	0.00011
CYP1B1	Hs00164383_m1	28	4	5.67	0.01420
GCLC	Hs00155249_m1	28	4	2.28	0.00708
NQO1	Hs00168547_m1	28	4	2.00	0.00195

To confirm the differential expression of a subset of mRNAs observed in the microarray analysis, RT-qPCR on the same RNA samples were performed. RT-qPCRs were conducted using the High-Capacity cDNA Reverse Transcription Kit and TaqMan Assay-on-Demand kits from Applied Biosystems (Darmstadt, Germany). The relative expression of the RNAs was determined by the comparative Ct method, where significance was assessed via an unpaired and 2-tailed *t*-test over 3 biological replicates. Expression values were first normalized to the control RNA (GAPDH) by using the equation $2^{-\Delta Ct}$ (with $\Delta Ct = Ct_{(target)} - Ct_{(control)}$). Then, the relative fold induction of the RNA in exposed tissue vs. control was calculated, and significance was assessed via an unpaired and 2-tailed *t*-test over 3 biological replicates. CS, cigarette smoke.

how this perturbation could later on lead to complex diseases like COPD or lung cancer represent an important challenge for the scientific community. This is especially true for these CS-associated lung diseases that are usually diagnosed at late stage, by which time it is not possible to reverse the damage done to the pulmonary tissue. For a long time, the characterization of CS biological effects at the cellular level was performed using immersed cell culture exposed not directly to whole CS but rather to part of it. CS was thus fractionate into total particulate matter, or gas vapor phase, or simply dissolved and diluted directly into the culture medium or any other solvent before being applied to the cells. Albeit practical, this approach unfortunately does not reflect an in vivo exposure, and only inhalation studies performed on animal models could offer the advantage of a direct whole CS exposure. However, due to species translatability issues and to the need for finding alternative models to reduce animal experiments, this in vivo approach also has its limitations.

The emergence of human three-dimensional airway epithelial tissue-like culture that can be maintained in vitro is thus a turning point in the field of environmental air pollutant risk assessment. The fact that these cultured primary cells can be directly exposed to any aerosol at the air-liquid interface is clearly a step forward in the development of a standard experimental airway model. Indeed, different studies demonstrated the relevance of this organotypic human bronchial epithelial cell culture to investigate normal biological processes occurring in the lung [e.g., mucus secretion (4, 52, 63)] as well as airway diseases mechanisms [asthma (18), COPD (55), CF (12, 50)]. Evidence showing that this in vitro airway model closely resembles the in vivo situation has also been provided at the morphological level (33) (see also Fig. 2) and more recently at the molecular level (46). Actually, in a healthy situation, this in vitro model reproduces important biological characteristics observed in a NHBE; when cultured at the air-liquid interface, NHBE cells differentiate into p63-positive basal cells, goblet cells, and ciliated and nonciliated cells and form a multilayered pseudo-stratified epithelium with typical mucociliary morphology. These various cell types expressed a similar gene expression pattern to the one observed in bronchial epithelial cells harvested directly from human pulmonary airway in vivo (46). They can thus recapitulate the specific biological characteristic necessary for their role of epithelial barrier in the lung (tight junctions, mucus clearance via cilia beating, or secretion of different factors, etc.).

The usefulness of the 3D culture model has already been proven (see the introduction), and we set out to assess what is happening when this cellular system is exposed to whole CS. More specifically, we wanted to see how closely this in vitro system can mimic the biological perturbations induced by CS inhalation in vivo in human airway epithelium. As first control for the responsiveness of our in vitro culture to CS, we showed a dose-dependent upregulation of pro-MMP-1 release by the AIR-100 tissue after CS exposure. This observation coincides well with the results of previous studies demonstrating that MMP-1 was upregulated in response to CS exposure both in vivo and in vitro (34, 36, 47) and on the identification of CS-regulatory elements in human MMP-1 promoter (38).

For the first in vitro/in vivo comparison, different in vivo smoking and smoking cessation gene signatures were extracted from published datasets corresponding to bronchial epithelial cells obtained from smokers (with current consumption or with low exposure to CS), nonsmokers, and former smokers, all healthy (3, 19, 56, 61, 71). For both smoking (current smokers vs. nonsmokers) and smoking cessation (former smokers vs. current smokers) gene signatures, the conserved gene overlap observed among these different in vivo datasets confirmed that CS-exposed bronchial epithelial cells express a similar gene expression profile despite different origin along the airway (large airways or small airways) (15, 19). Considering the variability induced in this type of analysis by the methodology (e.g., collection of samples, different chips), the heterogeneity of the group of donors, or the biological samples analyzed (e.g., cell type composition, biological states of the cells), it is remarkable to observe such similarity among different human datasets.

Using GSEA, we observed that all four in vivo smoking gene signatures were significantly enriched in the AIR-100 expression profiles. This resemblance was true for the directionality of the differentially regulated genes identified in the in vitro/in vivo comparison and was also stronger for the upregulated genes comparison than for the downregulated genes comparison. This latest observation may reflect differences between the effects of acute (in vitro situation) vs. chronic (in vivo situation) CS exposure. Significant normalized enrichment scores were observed after 2-h postexposure and were then sustained until 48 h with the highest score observed at 4-h postexposure time. Many of the biological functions known to be directly affected upon CS exposure, both in vivo and in vitro (7, 17, 37, 72), were identified based on the leading edge genes

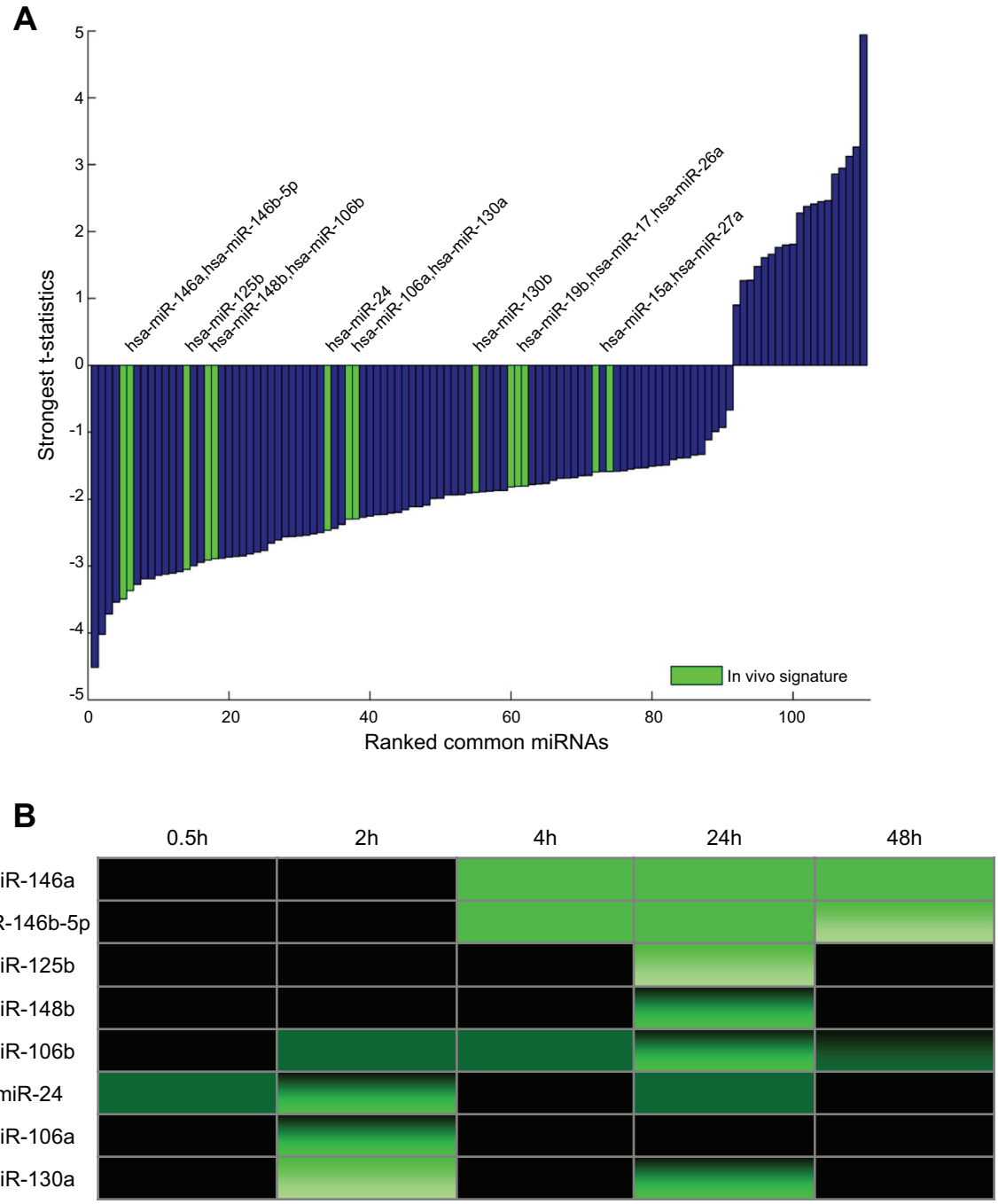

Fig. 7. Comparison between in vivo human smoker miRNA signature [from Schembri et al. (54)] and CS-exposed AIR-100 in vitro miRNA dataset. *A*: vertical axis of the bar plot represents the best *t*-statistics (i.e., lowest negative or highest positive *t*-scores) obtained for the coefficients β_t or β_i of the linear model. The 14 miRNAs detected by both platforms and contributing to the in vivo signature (highlighted in green) are all downregulated upon CS exposure. *B*: heatmap showing the different response kinetics of 8 CS-induced miRNAs expressed in AIR-100 tissue that correspond to the most significant element of the in vivo miRNA smoking signature. Vertical color gradients, responses dependent on exposure time; black, absence of response; green, downregulation in CS-exposed AIR-100 tissue vs. control.

that contribute to the highest enrichment score observed at 4-h postexposure. For instance, the metabolism of xenobiotics by cytochrome P450, the redox balance, the glutathione metabolism, the pentose phosphate pathway, and various solute transport genes were all highlighted by the functional analysis performed on the GSEA results. Direct targets of Nrf2 transcription factor were also found in the list of leading edge genes that contributed to the enrichment of the in vivo smoking gene signature (e.g., NQO1, TXNRD1, GCLM, ME1, TXN, GCLC, ABCC1, AKR1C1, FTH1, and FTL) in the in vitro CS-exposed AIR-100 expression profiles. Interestingly, genes related to Notch (DLL1, JAG2, MAML3, and HEY1) and WNT/β-catenin pathways (SOX9, RHOU, and RUNX2) were also identified in the list of downregulated genes matching both in vitro/in vivo expression profile. These results are in agreement with previous studies highlighting the effect of CS

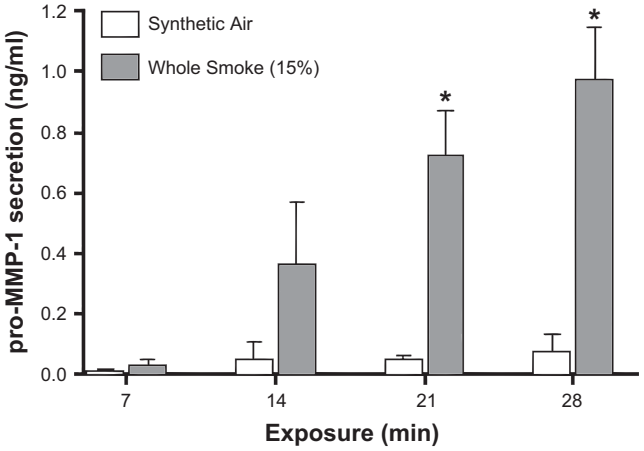

Fig. 8. Measurement of the basolateral secretion of pro-matrix metalloproteinase 1 (MMP-1) protein 48 h after various CS or air exposure times (7, 14, 21, 28 min) of AIR-100 tissue. A significant dose-dependent increase in MMP-1 secretion was seen after 14 min, 21 min, and 28 min of exposure to whole CS (up to 14-fold for 28-min exposure time) compared with sham. $*P < 0.01$, 1-way ANOVA and Tukey's multiple-comparison post hoc test, means ± SE, $N = 3$ replicates.

exposure on the downregulation of these pathways in human airway epithelium (64, 67). We also observed in the downregulated leading edge genes a certain number of family members of the apical junction complex molecules that are known to reduce the epithelial integrity after CS exposure. This observation was also reported by Heijink et al. (23) in their recently published in vivo and in vitro study.

Because the CS-exposed AIR-100 in vitro system recapitulates nicely the gene expression profiles observed in the bronchial epithelial cells of human smokers, we decided to investigate whether this resemblance was also occurring at the level of miRNA expression. Although only one study of the miRNA response to CS in in vivo human bronchial epithelial cells was available, the in vitro results presented here showed translatable global behaviors and pinpointed several miRNAs that reacted strongly in both cases. These results are very encouraging, given the various factors that differed between the two situations. The transcriptomics results described above showed that the AIR-100 system and the applied treatment are suitable for the reproduction of the in vivo cellular perturbations induced by CS inhalation in human bronchial epithelium. Two additional difficulties needed to be surmounted to reach similar conclusions based on miRNA expression profiles. First, the fact that the profiling platforms were not the same could lead to a distortion of the signal, as already observed when comparing different miRNA profiling platforms (53). Second, the number of miRNAs commonly detected on the two platforms was relatively small. This feature is favorable for the targeted detection of biomarker candidates because it is easier to handle a small number of candidates for subsequent biomarker validation such as the top five translatable miRNAs observed in Fig. 3. However, it becomes a problem at the level of the statistical power, especially when the signal-to-noise ratio of the data is low, which was the case in the miRNA measurements performed in this study. Indeed, the principal component analysis revealed that CS-induced variability accounted for only ~10% of the total variance (data not shown). Therefore the fact that some elements of the in vivo miRNA smoking signature displayed a moderate in vitro response may simply reflect this unfavorable context. In summary, despite some difficulties, the miRNA results are nevertheless strongly supportive of the in vitro/in vivo translatability of the CS effects. For instance, the observed downregulation of the expression of a large miRNA fraction reflects an effect that has been observed in vivo, not only in human bronchial epithelium (54), but also in the lungs of rat exposed to CS (31). The results obtained in vitro also reveal the different kinetics of miRNA responses (Fig. 7*B*). Globally they show that the changes are the strongest 24 h after CS exposure. Interestingly, the biological functions associated with the highly translatable miRNAs identified in this analysis are related to inflammation [e.g., miR-146b (41, 44, 45), miR-125b (75)] and cell cycle processes [e.g., miR-106a and miR-106b (22, 30, 32, 39, 57)] that are also known to be perturbed by CS in lung tissue context (37).

To conclude, NHBE cells differentiated in an organotypic culture and exposed to CS at the air-liquid interface represent a valuable tool that can be used to further understand the biological impact of CS on human lung epithelium. The possibility to mimic systems response profile occurring in a human smoker's bronchial epithelium offers the advantage to further detail the molecular processes perturbed by CS exposure.

It is important to mention that the short-term exposure presented here should be still considered as a pilot study and cannot be yet compared with pathological tissues such as those obtained from the lung of patients with COPD. Because the concentration of whole smoke tested here was set up to avoid exposure condition too toxic for the cells (monitoring of cell survival via resazurin assay), we did not investigate the apoptosis effect caused by CS. Thus evaluation of this in vitro system over longer periods in culture may be the next step in the process of investigating both chronic CS exposure and smoking cessation effects. It may also help to identify early events leading to the development of smoking-related airway pathologies. Furthermore, exploring the effect of CS in recently developed coculture assays could also be of interest. Recently, Pageau et al. (42) investigated the effect of altered communication between stromal and epithelial tissue compartments with a coculture system composed of a collagen matrix, lung fibroblasts, and a pseudo-stratified bronchial epithelium like the AIR-100 tissue. Knowing the important role of inflammatory cells in the response of the airway to airborne pollutants, the addition of inflammatory cells to this organotypic airway culture should be considered as the next essential step to further establish an in vitro model even more representative to key changes occurring in human lung after CS exposure and potentially leading to serious pathologies. Actually, it has been reported that human bronchial epithelial cells cultured at the air-liquid interface together with macrophages was feasible to study particle deposition impact (13) or to mimic lung responses to anthrax infection (49). Another approach to investigate the inflammatory component in the response to CS using this organotypic in vitro airway model could be to add in the culture medium proinflammatory molecules known to be released in smokers' lungs. Interestingly, a human lung-on-a-chip microdevice has been developed by the group of D. E. Ingber that mimics the alveolar-capillary barrier and reproduced breathing movement (27). They addressed the inflammatory component by inducing the activation of microvascular endothelium with TNF-α and by adding subsequently fluores-

cently labeled neutrophils to test their adherence to the endothelium. They also demonstrated that it was possible to mimic drug toxicity-induced pulmonary edema (26) with this new experimental model.

The optimization of human organotypic airway model to further match physiological context is still an important challenge. It will require additional comparison between in vivo and in vitro situation to further establish them as reliable alternatives to animal models or to two-dimensional culture. Finally, the combination of systems biology approaches together with such human organotypic airway culture will certainly open the way to further understand the cellular and molecular impact of air pollutants like CS.

ACKNOWLEDGMENTS

The authors thank Stéphanie Boue, Michael Peck, and Anthony Tricker for helpful discussion during the manuscript preparation. We also acknowledge the technical expertise of Christina Berger, Marek Franitza, Torsten Wilms, and Jessica Buechel for AIR100 mRNA sample processing and transcriptomics data generation, Sigrid Lufen for miRNA logistics, and Marco Hebestreit and Birgit Kurkowsky for all cell culture aspects of the study. We also thank Grégory Vuillaume for the Fleiss κ statistic calculation for the gene signature agreement analysis.

DISCLOSURES

No conflicts of interest, financial or otherwise, are declared by the authors.

AUTHOR CONTRIBUTIONS

Author contributions: C.M., C.P., D.W., A.H., S.W., J.H., and M.P. conception and design of research; C.M., C.P., D.W., S.G., A.H., A.S., V.B., Y.X., and S.A. analyzed data; C.M., C.P., D.W., S.G., A.H., A.S., V.B., and Y.X. interpreted results of experiments; C.M., C.P., D.W., A.S., and V.B. prepared figures; C.M., C.P., D.W., S.G., A.H., A.S., V.B., Y.X., and S.A. drafted manuscript; C.M., C.P., S.G., A.S., and J.H. edited and revised manuscript; C.M., C.P., S.G., J.H., and M.P. approved final version of manuscript; D.W. and S.W. performed experiments.

REFERENCES

1. **Academies NRCotN.** *Toxicity Testing in the 21st Century: A Vision and a Strategy*. Washington, D.C.: The National Academies Press, 2007.
2. **Balharry D, Sexton K, Berube KA.** An in vitro approach to assess the toxicity of inhaled tobacco smoke components: nicotine, cadmium, formaldehyde and urethane. *Toxicology* 244: 66–76, 2008.
3. **Beane J, Sebastiani P, Liu G, Brody JS, Lenburg ME, Spira A.** Reversible and permanent effects of tobacco smoke exposure on airway epithelial gene expression. *Genome Biol* 8: R201, 2007.
4. **Bernacki SH, Nelson AL, Abdullah L, Sheehan JK, Harris A, Davis CW, Randell SH.** Mucin gene expression during differentiation of human airway epithelia in vitro. Muc4 and muc5b are strongly induced. *Am J Respir Cell Mol Biol* 20: 595–604, 1999.
5. **Booth BW, Sandifer T, Martin EL, Martin LD.** IL-13-induced proliferation of airway epithelial cells: mediation by intracellular growth factor mobilization and ADAM17. *Respir Res* 8: 51, 2007.
6. **Chen C, Grennan K, Badner J, Zhang D, Gershon E, Jin L, Liu C.** Removing batch effects in analysis of expression microarray data: an evaluation of six batch adjustment methods. *PLoS One* 6: e17238, 2011.
7. **Comandini A, Marzano V, Curradi G, Federici G, Urbani A, Saltini C.** Markers of anti-oxidant response in tobacco smoke exposed subjects: a data-mining review. *Pulm Pharmacol Ther* 23: 482–492, 2010.
8. **Commission E.** Alternative Testing Strategies: Progress report *2009: Replacing, Reducing and Refining Use of Animals in Research: Genomics & Biotechnology for Health*. Luxembourg, Luxembourg: Office for Official Publications of the European Communities, 2009.
9. **Cortes C, Vapnik V.** Support-vector networks. *Mach Learn* 20: 273–297, 1995.
10. **Culpitt SV, Rogers DF, Traves SL, Barnes PJ, Donnelly LE.** Sputum matrix metalloproteases: comparison between chronic obstructive pulmonary disease and asthma. *Respir Med* 99: 703–710, 2005.
11. **Dechecchi MC, Nicolis E, Mazzi P, Cioffi F, Bezzerri V, Lampronti I, Huang S, Wiszniewski L, Gambari R, Scupoli MT, Berton G, Cabrini G.** Modulators of sphingolipid metabolism reduce lung inflammation. *Am J Respir Cell Mol Biol* 45: 825–833, 2011.
12. **Derichs N, Jin BJ, Song Y, Finkbeiner WE, Verkman AS.** Hyperviscous airway periciliary and mucous liquid layers in cystic fibrosis measured by confocal fluorescence photobleaching. *FASEB J* 25: 2325–2332, 2011.
13. **Diabate S, Mulhopt S, Paur HR, Krug HF.** The response of a co-culture lung model to fine and ultrafine particles of incinerator fly ash at the air-liquid interface. *Altern Lab Anim* 36: 285–298, 2008.
14. **Fleiss JL, Levin B, Paik MC.** *Statistical Methods for Rates and Proportions*. Hoboken, NJ: John Willey & Sons, 2003.
15. **Gower AC, Steiling K, Brothers JF 2nd, Lenburg ME, Spira A.** Transcriptomic studies of the airway field of injury associated with smoking-related lung disease. *Proc Am Thorac Soc* 8: 173–179, 2011.
16. **Gruenert DC, Finkbeiner WE, Widdicombe JH.** Culture and transformation of human airway epithelial cells. *Am J Physiol Lung Cell Mol Physiol* 268: L347–L360, 1995.
17. **Hackett NR, Heguy A, Harvey BG, O'Connor TP, Luettich K, Flieder DB, Kaplan R, Crystal RG.** Variability of antioxidant-related gene expression in the airway epithelium of cigarette smokers. *Am J Respir Cell Mol Biol* 29: 331–343, 2003.
18. **Hackett TL, Singhera GK, Shaheen F, Hayden P, Jackson GR, Hegele RG, Van Eeden S, Bai TR, Dorscheid DR, Knight DA.** Intrinsic phenotypic differences of asthmatic epithelium and its inflammatory responses to rsv and air pollution. *Am J Respir Cell Mol Biol* 45: 1090–1100, 2011.
19. **Harvey BG, Heguy A, Leopold PL, Carolan BJ, Ferris B, Crystal RG.** Modification of gene expression of the small airway epithelium in response to cigarette smoking. *J Mol Med* 85: 39–53, 2007.
21. **Harvey PR, Tarran R, Garoff S, Myerburg MM.** Measurement of the airway surface liquid volume with simple light refraction microscopy. *Am J Respir Cell Mol Biol* 45: 592–599, 2011.
22. **Hayashita Y, Osada H, Tatematsu Y, Yamada H, Yanagisawa K, Tomida S, Yatabe Y, Kawahara K, Sekido Y, Takahashi T.** A polycistronic microRNA cluster, miR-17–92, is overexpressed in human lung cancers and enhances cell proliferation. *Cancer Res* 65: 9628–9632, 2005.
23. **Heijink IH, Brandenburg SM, Postma DS, van Oosterhout AJ.** Cigarette smoke impairs airway epithelial barrier function and cell-cell contact recovery. *Eur Respir J* 39: 419–428, 2011.
24. **Henke MO, Renner A, Rubin BK, Gyves JI, Lorenz E, Koo JS.** Up-regulation of S100A8 and S100A9 protein in bronchial epithelial cells by lipopolysaccharide. *Exp Lung Res* 32: 331–347, 2006.
25. **Hou L, Wang D, Baccarelli A.** Environmental chemicals and microRNAs. *Mutat Res* 714: 105–112, 2011.
26. **Huh D, Leslie DC, Matthews BD, Fraser JP, Jurek S, Hamilton GA, Thorneloe KS, McAlexander MA, Ingber DE.** A human disease model of drug toxicity-induced pulmonary edema in a lung-on-a-chip microdevice. *Sci Transl Med* 4: 159ra147, 2012.
27. **Huh D, Matthews BD, Mammoto A, Montoya-Zavala M, Hsin HY, Ingber DE.** Reconstituting organ-level lung functions on a chip. *Science* 328: 1662–1668, 2010.
28. **Huntzinger E, Izaurralde E.** Gene silencing by microRNAs: contributions of translational repression and mRNA decay. *Nat Rev Genet* 12: 99–110, 2011.
29. **Iorio F, Bosotti R, Scacheri E, Belcastro V, Mithbaokar P, Ferriero R, Murino L, Tagliaferri R, Brunetti-Pierri N, Isacchi A, di Bernardo D.** Discovery of drug mode of action and drug repositioning from transcriptional responses. *Proc Natl Acad Sci USA* 107: 14621–14626, 2010.
30. **Ivanovska I, Ball AS, Diaz RL, Magnus JF, Kibukawa M, Schelter JM, Kobayashi SV, Lim L, Burchard J, Jackson AL, Linsley PS, Cleary MA.** MicroRNAs in the miR-106b family regulate p21/CDKN1A and promote cell cycle progression. *Mol Cell Biol* 28: 2167–2174, 2008.
31. **Izzotti A, Calin GA, Arrigo P, Steele VE, Croce CM, De Flora S.** Downregulation of microRNA expression in the lungs of rats exposed to cigarette smoke. *FASEB J* 23: 806–812, 2009.
32. **Jiang Y, Wu Y, Greenlee AR, Wu J, Han Z, Li X, Zhao Y.** miR-106a-mediated malignant transformation of cells induced by anti-benzo[a]pyrene-trans-7,8-diol-9,10-epoxide. *Toxicol Sci* 119: 50–60, 2011.

33. **Karp PH, Moninger TO, Weber SP, Nesselhauf TS, Launspach JL, Zabner J, Welsh MJ.** An in vitro model of differentiated human airway epithelia. Methods for establishing primary cultures. *Methods Mol Biol* 188: 115–137, 2002.
34. **Lahmann C, Bergemann J, Harrison G, Young AR.** Matrix metalloproteinase-1 and skin ageing in smokers. *Lancet* 357: 935–936, 2001.
35. **Maunders H, Patwardhan S, Phillips J, Clack A, Richter A.** Human bronchial epithelial cell transcriptome: gene expression changes following acute exposure to whole cigarette smoke in vitro. *Am J Physiol Lung Cell Mol Physiol* 292: L1248–L1256, 2007.
36. **Mercer BA, Kolesnikova N, Sonett J, D'Armiento J.** Extracellular regulated kinase/mitogen activated protein kinase is up-regulated in pulmonary emphysema and mediates matrix metalloproteinase-1 induction by cigarette smoke. *J Biol Chem* 279: 17690–17696, 2004.
37. **Mercer BA, Lemaitre V, Powell CA, D'Armiento J.** The epithelial cell in lung health and emphysema pathogenesis. *Curr Respir Med Rev* 2: 101–142, 2006.
38. **Mercer BA, Wallace AM, Brinckerhoff CE, D'Armiento JM.** Identification of a cigarette smoke-responsive region in the distal MMP-1 promoter. *Am J Respir Cell Mol Biol* 40: 4–12, 2009.
39. **Navarro A, Marrades RM, Vinolas N, Quera A, Agusti C, Huerta A, Ramirez J, Torres A, Monzo M.** MicroRNAs expressed during lung cancer development are expressed in human pseudoglandular lung embryogenesis. *Oncology* 76: 162–169, 2009.
40. **O'Brien J, Wilson I, Orton T, Pognan F.** Investigation of the Alamar Blue (resazurin) fluorescent dye for the assessment of mammalian cell cytotoxicity. *Eur J Biochem* 267: 5421–5426, 2000.
41. **O'Neill LA, Sheedy FJ, McCoy CE.** MicroRNAs: the fine-tuners of Toll-like receptor signalling. *Nat Rev Immunol* 11: 163–175, 2011.
42. **Pageau SC, Sazonova OV, Wong JY, Soto AM, Sonnenschein C.** The effect of stromal components on the modulation of the phenotype of human bronchial epithelial cells in 3D culture. *Biomaterials* 32: 7169–7180, 2011.
43. **Pedemonte CH.** Inhibition of Na(+)-pump expression by impairment of protein glycosylation is independent of the reduced sodium entry into the cell. *J Membr Biol* 147: 223–231, 1995.
44. **Perry MM, Moschos SA, Williams AE, Shepherd NJ, Larner-Svensson HM, Lindsay MA.** Rapid changes in microRNA-146a expression negatively regulate the IL-1beta-induced inflammatory response in human lung alveolar epithelial cells. *J Immunol* 180: 5689–5698, 2008.
45. **Perry MM, Williams AE, Tsitsiou E, Larner-Svensson HM, Lindsay MA.** Divergent intracellular pathways regulate interleukin-1beta-induced miR-146a and miR-146b expression and chemokine release in human alveolar epithelial cells. *FEBS Lett* 583: 3349–3355, 2009.
46. **Pezzulo AA, Starner TD, Scheetz TE, Traver GL, Tilley AE, Harvey BG, Crystal RG, McCray PB Jr, Zabner J.** The air-liquid interface and use of primary cell cultures are important to recapitulate the transcriptional profile of in vivo airway epithelia. *Am J Physiol Lung Cell Mol Physiol* 300: L25–L31, 2011.
47. **Phillips J, Kluss B, Richter A, Massey E.** Exposure of bronchial epithelial cells to whole cigarette smoke: assessment of cellular responses. *Altern Lab Anim* 33: 239–248, 2005.
48. **Putnam KP, Bombick DW, Doolittle DJ.** Evaluation of eight in vitro assays for assessing the cytotoxicity of cigarette smoke condensate. *Toxicol In Vitro* 16: 599–607, 2002.
49. **Radyuk SN, Mericko PA, Popova TG, Grene E, Alibek K.** In vitro-generated respiratory mucosa: a new tool to study inhalational anthrax. *Biochem Biophys Res Commun* 305: 624–632, 2003.
50. **Randell SH, Fulcher ML, O'Neal W, Olsen JC.** Primary epithelial cell models for cystic fibrosis research. *Methods Mol Biol* 742: 285–310, 2011.
51. **Ritchie ME, Silver J, Oshlack A, Holmes M, Diyagama D, Holloway A, Smyth GK.** A comparison of background correction methods for two-colour microarrays. *Bioinformatics* 23: 2700–2707, 2007.
52. **Ross AJ, Dailey LA, Brighton LE, Devlin RB.** Transcriptional profiling of mucociliary differentiation in human airway epithelial cells. *Am J Respir Cell Mol Biol* 37: 169–185, 2007.
53. **Sato F, Tsuchiya S, Terasawa K, Tsujimoto G.** Intra-platform repeatability and inter-platform comparability of microRNA microarray technology. *PLoS One* 4: e5540, 2009.
54. **Schembri F, Sridhar S, Perdomo C, Gustafson AM, Zhang X, Ergun A, Lu J, Liu G, Bowers J, Vaziri C, Ott K, Sensinger K, Collins JJ, Brody JS, Getts R, Lenburg ME, Spira A.** MicroRNAs as modulators of smoking-induced gene expression changes in human airway epithelium. *Proc Natl Acad Sci USA* 106: 2319–2324, 2009.
55. **Schneider D, Ganesan S, Comstock AT, Meldrum CA, Mahidhara R, Goldsmith AM, Curtis JL, Martinez FJ, Hershenson MB, Sajjan U.** Increased cytokine response of rhinovirus-infected airway epithelial cells in chronic obstructive pulmonary disease. *Am J Respir Crit Care Med* 182: 332–340, 2010.
56. **Shaykhiev R, Otaki F, Bonsu P, Dang DT, Teater M, Strulovici-Barel Y, Salit J, Harvey BG, Crystal RG.** Cigarette smoking reprograms apical junctional complex molecular architecture in the human airway epithelium in vivo. *Cell Mol Life Sci* 68: 877–892, 2011.
57. **Shen YL, Jiang YG, Greenlee AR, Zhou LL, Liu LH.** MicroRNA expression profiles and miR-10a target in anti-benzo[a] pyrene-7, 8-diol-9, 10-epoxide-transformed human 16HBE cells. *Biomed Environ Sci* 22: 14–21, 2009.
58. **Smyth GK.** Limma: linear models for microarray data. In: *Bioinformatics and Computational Biology Solutions Using R and Bioconductor*, edited by Gentleman R, Carey V, Huber W, Irizarry RA and Duboit S. Washington, DC: Springer, 2005, p. 397–420.
59. **Smyth GK.** Linear models and empirical bayes methods for assessing differential expression in microarray experiments. *Stat Appl Genet Mol Biol* 3: Article3, 2004.
60. **Spira A, Beane J, Shah V, Liu G, Schembri F, Yang X, Palma J, Brody JS.** Effects of cigarette smoke on the human airway epithelial cell transcriptome. *Proc Natl Acad Sci USA* 101: 10143–10148, 2004.
61. **Strulovici-Barel Y, Omberg L, O'Mahony M, Gordon C, Hollmann C, Tilley AE, Salit J, Mezey J, Harvey BG, Crystal RG.** Threshold of biologic responses of the small airway epithelium to low levels of tobacco smoke. *Am J Respir Crit Care Med* 182: 1524–1532, 2010.
62. **Subramanian A, Tamayo P, Mootha VK, Mukherjee S, Ebert BL, Gillette MA, Paulovich A, Pomeroy SL, Golub TR, Lander ES, Mesirov JP.** Gene set enrichment analysis: a knowledge-based approach for interpreting genome-wide expression profiles. *Proc Natl Acad Sci USA* 102: 15545–15550, 2005.
63. **Tanabe T, Fujimoto K, Yasuo M, Tsushima K, Yoshida K, Ise H, Yamaya M.** Modulation of mucus production by interleukin-13 receptor alpha2 in the human airway epithelium. *Clin Exp Allergy* 38: 122–134, 2008.
64. **Tilley AE, Harvey BG, Heguy A, Hackett NR, Wang R, O'Connor TP, Crystal RG.** Down-regulation of the notch pathway in human airway epithelium in association with smoking and chronic obstructive pulmonary disease. *Am J Respir Crit Care Med* 179: 457–466, 2009.
65. **Tomankova T, Petrek M, Kriegova E.** Involvement of microRNAs in physiological and pathological processes in the lung. *Respir Res* 11: 159, 2010.
66. **Tusher VG, Tibshirani R, Chu G.** Significance analysis of microarrays applied to the ionizing radiation response. *Proc Natl Acad Sci USA* 98: 5116–5121, 2001.
67. **Wang R, Ahmed J, Wang G, Hassan I, Strulovici-Barel Y, Hackett NR, Crystal RG.** Down-regulation of the canonical Wnt beta-catenin pathway in the airway epithelium of healthy smokers and smokers with COPD. *PLoS One* 6: e14793, 2011.
68. **Watson AM, Benton AS, Rose MC, Freishtat RJ.** Cigarette smoke alters tissue inhibitor of metalloproteinase 1 and matrix metalloproteinase 9 levels in the basolateral secretions of human asthmatic bronchial epithelium in vitro. *J Investig Med* 58: 725–729, 2010.
69. **Whitcutt MJ, Adler KB, Wu R.** A biphasic chamber system for maintaining polarity of differentiation of cultured respiratory tract epithelial cells in vitro. *Cell Dev Biol* 24: 420–428, 1988.
70. **Yamaya M, Finkbeiner WE, Chun SY, Widdicombe JH.** Differentiated structure and function of cultures from human tracheal epithelium. *Am J Physiol Lung Cell Mol Physiol* 262: L713–L724, 1992.
71. **Zhang L, Lee JJ, Tang H, Fan YH, Xiao L, Ren H, Kurie J, Morice RC, Hong WK, Mao L.** Impact of smoking cessation on global gene expression in the bronchial epithelium of chronic smokers. *Cancer Prev Res (Phila)* 1: 112–118, 2008.
72. **Zhang X, Sebastiani P, Liu G, Schembri F, Dumas YM, Langer EM, Alekseyev Y, O'Connor GT, Brooks DR, Lenburg ME, Spira A.** Similarities and differences between smoking-related gene expression in nasal and bronchial epithelium. *Physiol Genomics* 41: 1–8, 2010.
73. **Zhao J, Maskrey B, Balzar S, Chibana K, Mustovich A, Hu H, Trudeau JB, O'Donnell V, Wenzel SE.** Interleukin-13-induced MUC5AC is regulated by 15-lipoxygenase 1 pathway in human bronchial epithelial cells. *Am J Respir Crit Care Med* 179: 782–790, 2009.

74. **Zhijin W, Irizarry RA, Gentleman R, Martinez Murillo F, Spencer F.** A model based background adjustement for oligonucleotide expression arrays. In: *Working Paper 1*. Baltimore: John Hopkins University, 2004.
75. **Zhou R, Hu G, Gong AY, Chen XM.** Binding of NF-kappaB p65 subunit to the promoter elements is involved in LPS-induced transactivation of miRNA genes in human biliary epithelial cells. *Nucleic Acids Res* 38: 3222–3232, 2010.
76. **Zimmermann GS, Neurohr C, Villena-Hermoza H, Hatz R, Behr J.** Anti-inflammatory effects of antibacterials on human Bronchial epithelial cells. *Respir Res* 10: 89, 2009.